Supplementary Information

Influences and Mechanism of Additives on Polymorphic Manipulation of Organic Fluorescent Crystals

Xiunan Zhang [a], Jingkang Wang [a,b], Fei Yu [a], Xiaowei Cheng [a], Yunhui Hao [a], Yue Liu [a], Xin Huang [a,b], Ting Wang [a,b*], and Hongxun Hao [a,b*]

[a] National Engineering Research Center of Industrial Crystallization Technology, School of Chemical Engineering and Technology, Tianjin University, Tianjin 300072, China
[b] Collaborative Innovation Center of Chemical Science and Engineering (Tianjin), Tianjin, 300072, China

## Contents

Experimental section

1.2. Synthesis Procedure. BMeTTPAL was readily synthesized by the Jones oxidation[1] and the following Suzuki-Miyaura coupling[2] (**Scheme S1**). The model compound was characterized and confirmed by 400 MHz ^{1}H and 100 MHz ^{13}C spectroscopy (Bruker AVANCE III) and high-resolution mass spectroscopy (HRMS, 1290 UPLC (Agilent)/ micrOTOF-Q II (Bruker)).
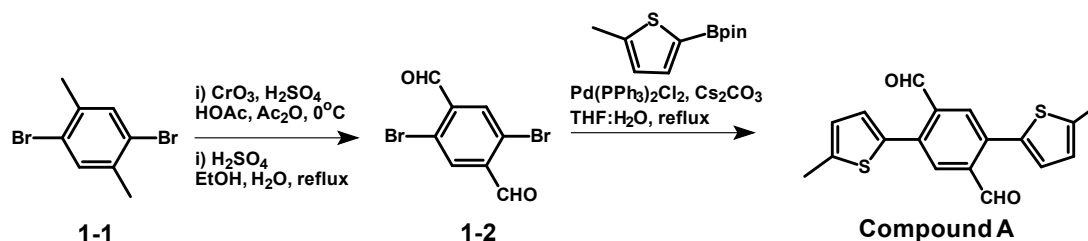

Scheme S1. Synthesis of compound A.

Preparation of **1-2** by Jones oxidation [1]: acetic acid (20.0 mL), acetic anhydride (40.0 mL) and 1,4-dibromo-2,5-dimethylbenzene (**1-1**, 4.0 g, 0.015 mol, 1.00 eq.) were added in a flask, then the sulfuric acid (14.0 mL) was added dropwise to this mixture and stirred at 0 °C. New grinding CrO_3 (6.0 g, 0.06 mol, 4.00 eq.) was slowly added in portions and stirred vigorously for another 5 hours at 0 °C. After the reaction finished, poured the greenish slurry into ice-water bath and filtered. The filter residue was further washed with ice water and cold methanol (about -15 °C). Then, the intermediate was carried on hydrolysis reaction under refluxing condition. The relevant solvents are ethanol (20.0 mL), water (20.0 mL) and sulfuric acid (2.0 mL). After cooling the reaction to 0 °C, the crude 1-2 was separated by filtration. The pure product was obtained by recrystallization from chloroform in 35% yield.

Preparation of compound A by a Suzuki-Miyaura cross coupling[2]: **1-2** (146 mg, 0.50 mmol, 0.50 eq.), $Pd(PPh_3)_2Cl_2$ (17.5 mg, 0.03 mmol, 0.03 eq.), substituted-thiophene-2-boronic acid pinacol ester (1.25 mmol, 1.25 eq.) and 1.0 mLCs_2CO_3 (0.82 g, 2.50 mmol, 2.50 eq.) solution (2M) in 5.0 mL dry THF were refluxed 48 hours under an nitrogen atmosphere. After finished, the mixture was extracted with ethyl acetate. The organic phase was further washed with saturated NaCl solution, water and dried with anhydrous Mg_2SO_4. The product was obtained by flash column chromatography or recrystallization in acetone with 85% yield. ^{1}H NMR (400 MHz, $CDCl_3$) δ = 10.27 (s, 2H), 8.08 (s, 2H), 6.91 (d, J=3.5, 2H), 6.83 (dd, J=3.5, 1.1, 2H), 2.57 (d, J=0.9, 6H). ^{13}C NMR (101 MHz, $CDCl_3$) δ = 191.44, 143.32, 136.88, 136.62, 135.06, 130.56, 130.09, 126.42, 15.40. HRMS (m/z): [M+H]$^+$ calcd for $C_{18}H_{14}O_2S_2Na$ 349.0333, found 349.0312.
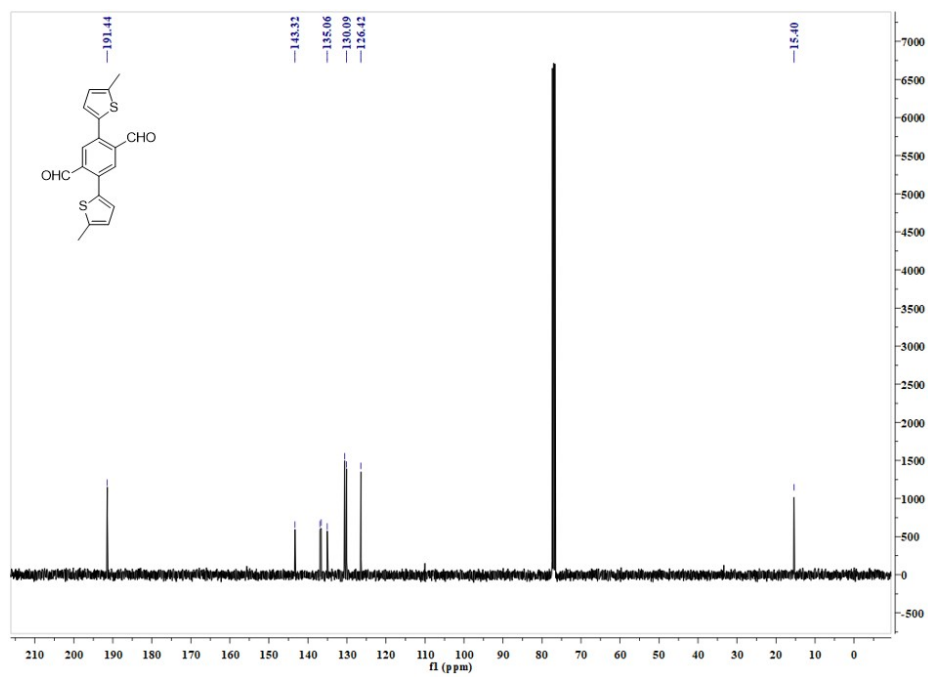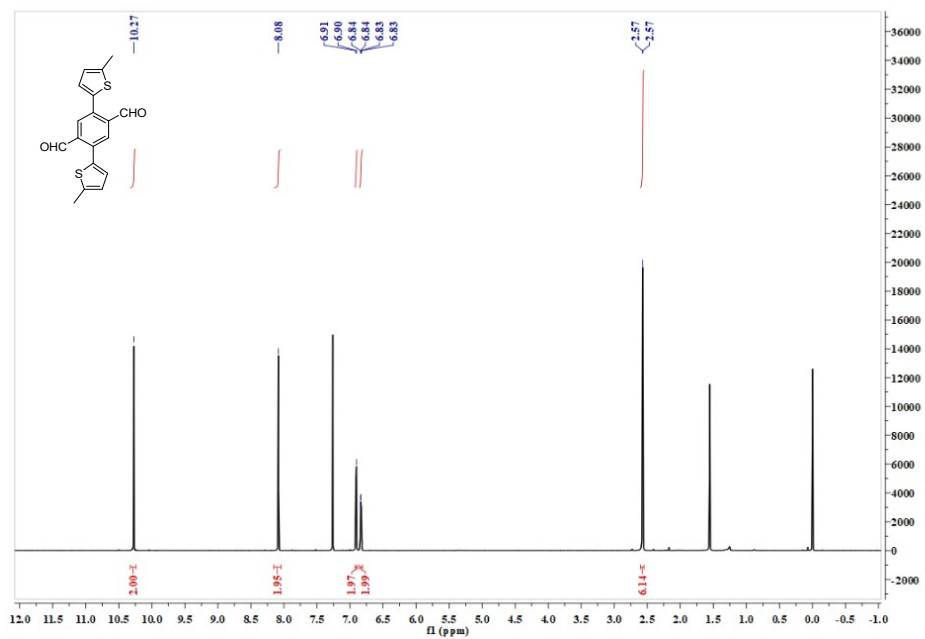
Fig. S1 ^{1}H NMR and ^{13}C NMR spectrum of 2,5-Bis(5-methyl-2-thienyl)terephthalaldehyde.
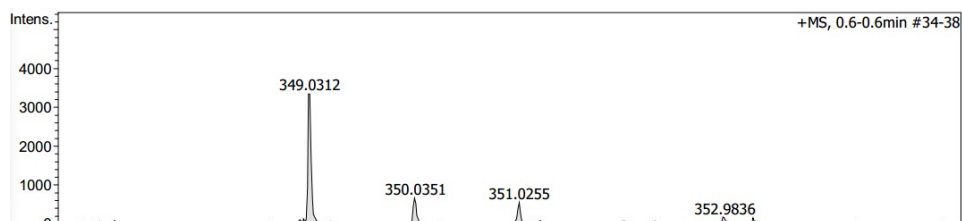
Fig. S2 High-resolution mass spectrometry (HRMS) spectra of 2,5-Bis(5-methyl-2-thienyl)terephthalaldehyde .
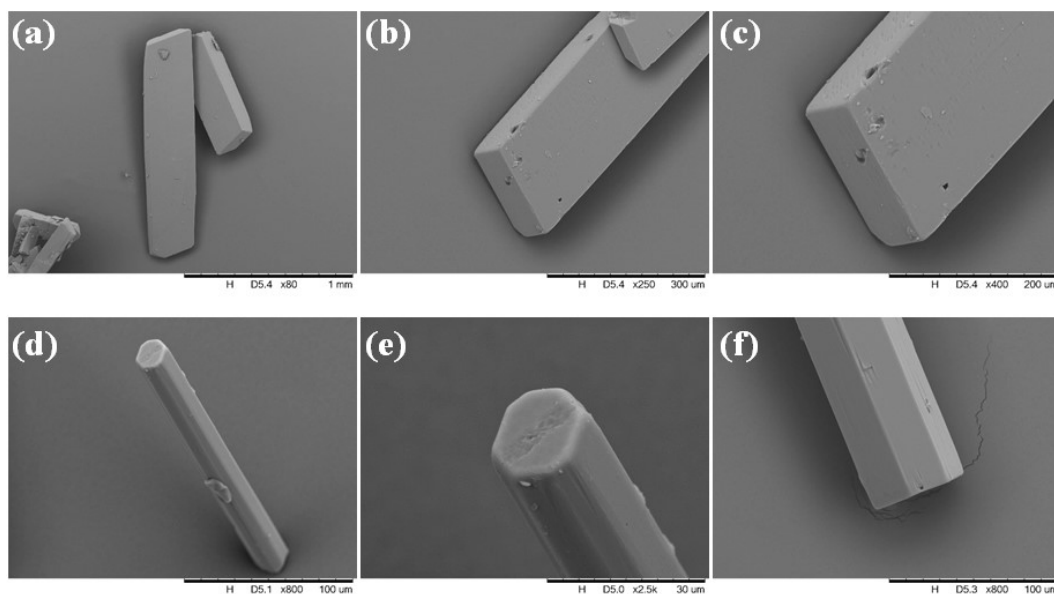
Morphology and Photophysical properties.

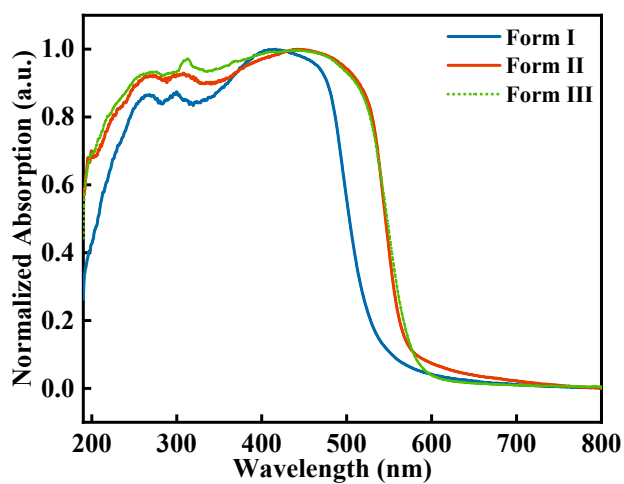**Fig. S3**. (a-c) The SEM images of Form I; (d-f) The SEM images of Form II.

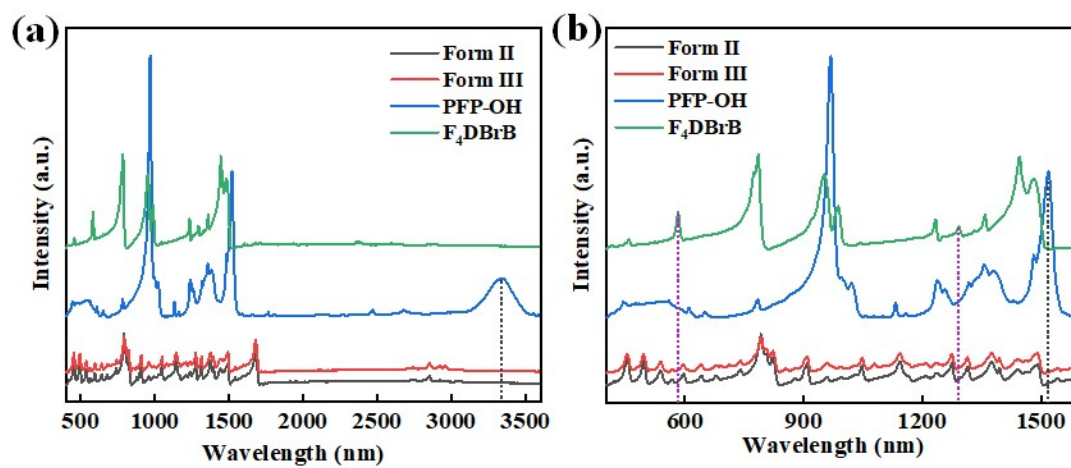**Fig. S4.** Normalized UV-vis absorption of Form I, Form II and Form III.

Fig. S5. (a) The FTIR spectra of Form II, Form III and additives; (b) The enlarged graphs of (a).
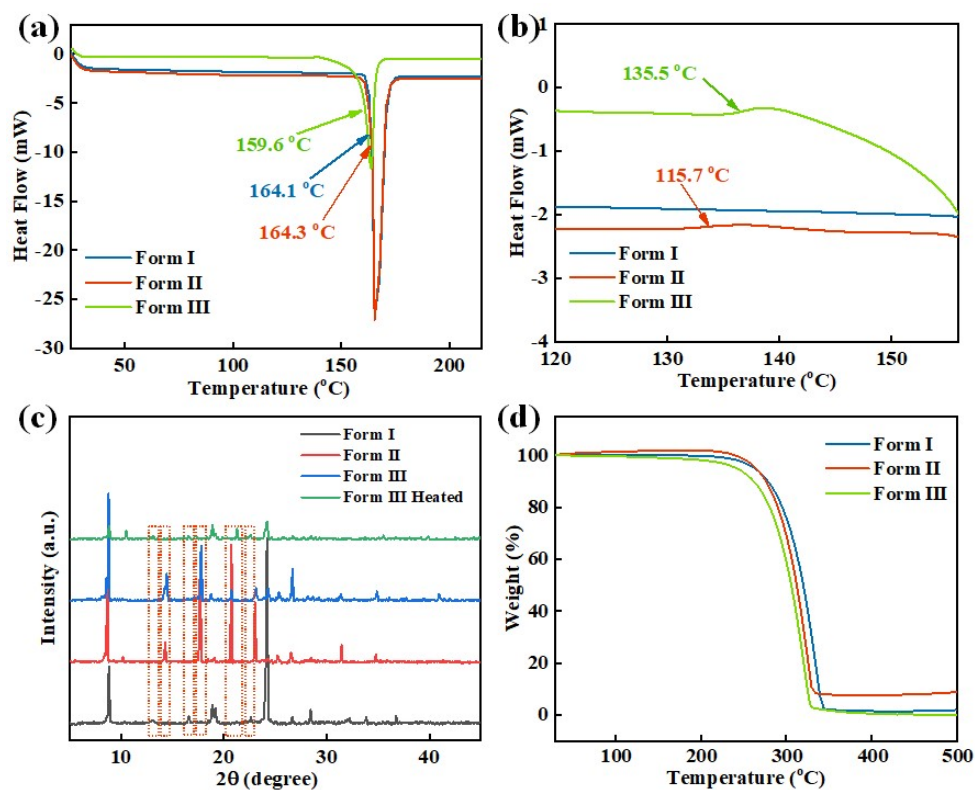
Fig. S6. (a) DSC plot of three polymorphs; (b) The enlarged image between 120 °C and 155 °C of the DSC plot; (c) The PXRD patterns of different polymorphs: Form I (grey), Form II (red), Form III (blue) and heated powder of FIII (green).
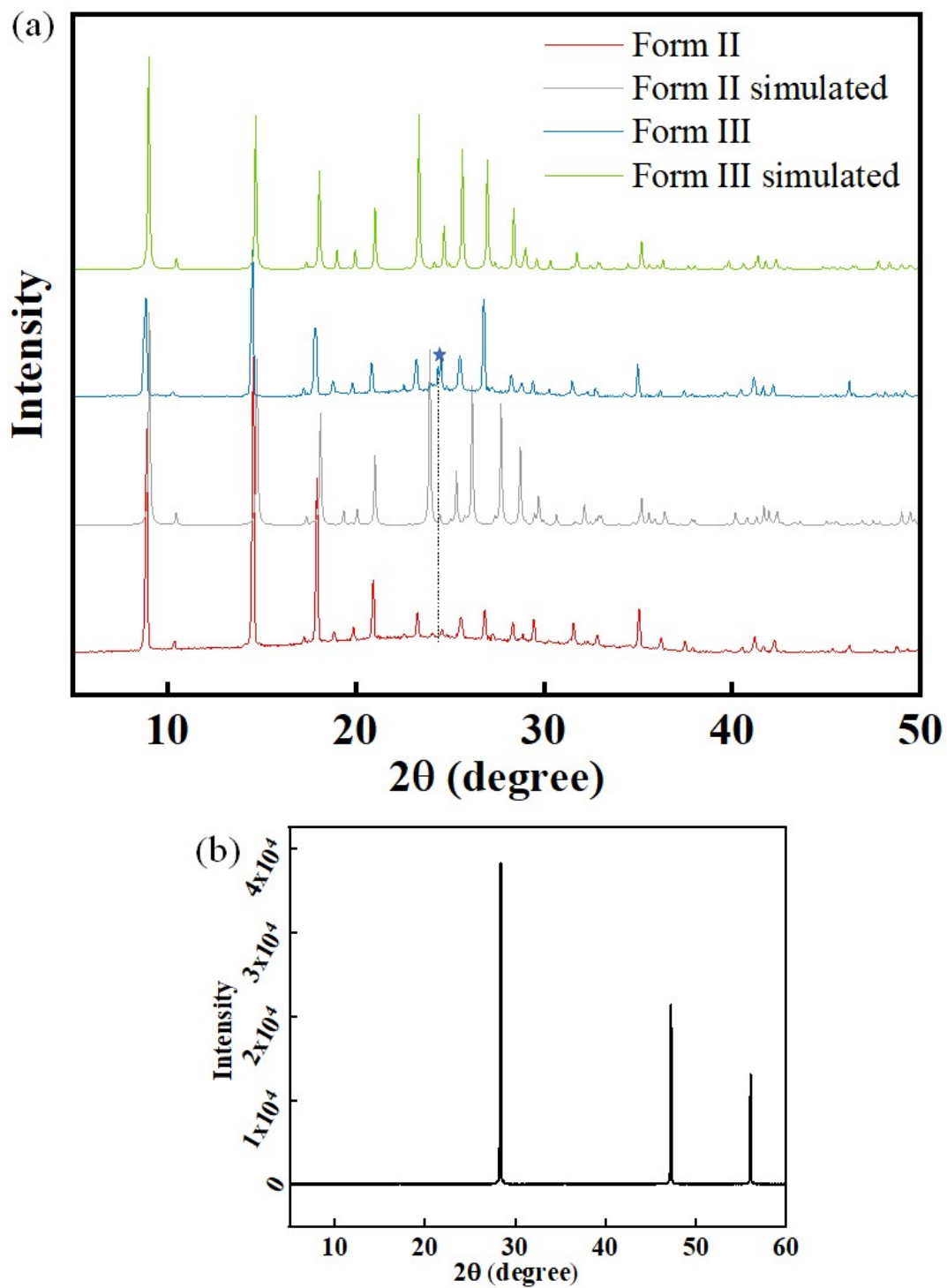
Fig. S7. (a) The simulation and experimental comparison diagram of Form II and Form III; (b) the PXRD diagram of standard sample of silicon crystal powder under the same condition of (a).

Table S1. The main PXRD data of Form II and Form III under experimental condition.

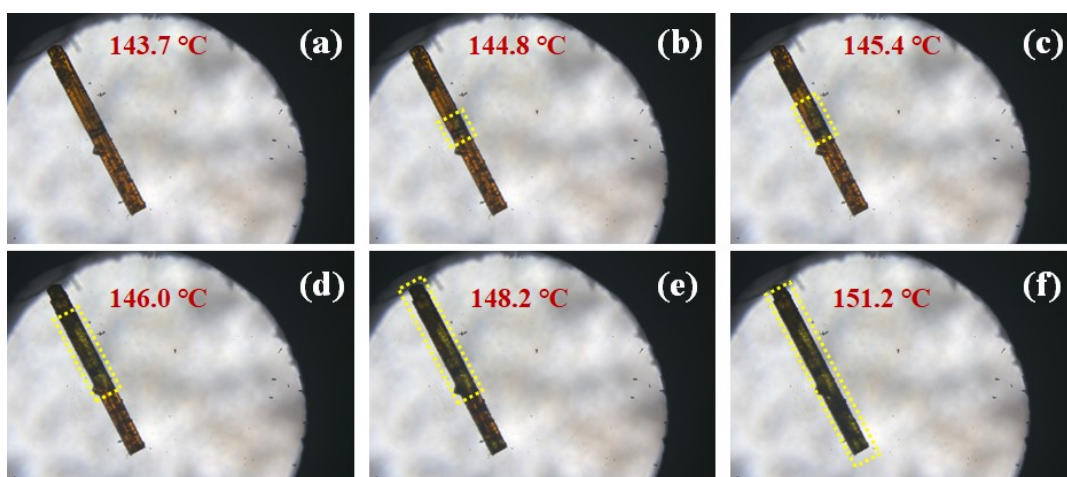| Form II (°)	Form III (°)	Δ
8.900	8.850	0.050
14.560	14.510	0.050
17.940	17.840	0.100
20.920	20.820	0.100
23.270	23.220	0.050
	24.360	
24.580	24.530	0.050
25.590	25.540	0.050
26.850	26.800	0.050
28.340	28.241	0.099
35.040	34.970	0.070

Note: Δ = Form II (°) – Form III (°); Experimental condition: 7 ℃ min^{-1}; The process was carried on from 5° to 60° with a step size of 0.01°, 7 ℃ min^{-1}, voltage of 40 kV, and current of 15 mA.

Table S2. The PXRD data of standard sample of silicon crystal powder under calibration condition and experimental condition.

Label	Theory (°)	Calibration condition (°)	Δ$_1$	Experimental condition (°)	Δ$_2$
Si (111)	28.401	28.403	-0.002	28.390	0.011
Si (220)	47.264	47.249	0.015	47.260	0.004
Si (311)	56.083	56.068	0.015	56.079	0.004
Si (400)	69.090	69.071	0.019		
Si (331)	76.336	76.315	0.021		
Si (422)	87.990	87.970	0.022		
Si (511)	94.912	94.888	0.024		
Si (440)	106.670	106.641	0.029		
Si (531)	114.055	114.024	0.030		
Si (620)	127.510	127.473	0.037		
Si (533)	136.861	136.819	0.042		

Note: Δ$_1$ = Theory (°) - Calibration condition (°); Δ$_2$= Theory (°) - Experimental condition (°); Experimental condition: The process was carried on from 5° to 60° with a step size of 0.01°, 7 ℃ min^{-1}, voltage of 40 kV, and current of 15 mA.

Fig. S8. The hot-stage microscopic graphs about the process of crystal transformation between Form III and Form I.

Table S3. The summary of crystallization conditions.

Crystalization Methods	Additives	Form I	Form II	Form III
Evaporation	F_4DBrB >=70% (w/w)	X	O	X
	PFP-OH >=10% (w/w)	X	O	X
	None	O	X	X
Cooling 5 ˚C/h	F_4DBrB >=30% (w/w)	X	O	X
	PFP-OH >=5% (w/w)	X	O	X
	None	O	X	X
Cooling 15 ˚C/h	None	X	O	X
Sublimition Under Vacuum		X	X	O

Note: The solvent for solution crystallization is acetone. The symbol X means not present and the character O means present.

**Molecule packing of Form I and Form II of BMeTTPAL.**
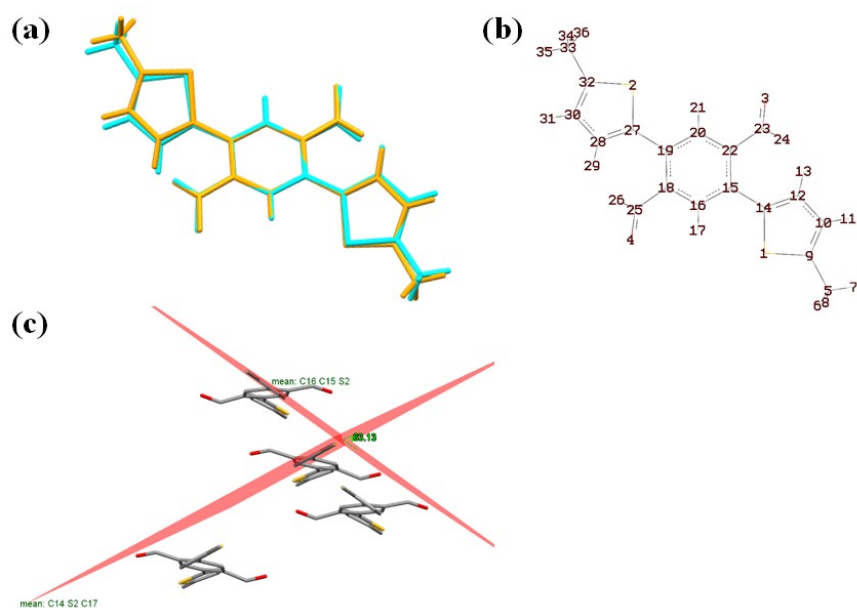
Fig. S9 (a) Overlay of the molecular conformations of Form I (cyan) and Form II (orange) in the solid state; (b) Atomic labels of BMeTTPAL molecule. (c) The dihedral angle between the substituted thiophene rings of neighboring molecules.[3]

Table S4. Crystallographic data of different polymorph of BMeTTPAL.

cell parameters	Form I[1]	Form II[3]	Form III
formula	$C_{18} H_{14} O_2 S_2$	$C_9 H_7 OS$	$C_{18} H_{14} O_2 S_2$
formula mass	326.41	163.21	326.41
crystal system	monoclinic	monoclinic	monoclinic
space group	C c	I2/a	C2/c
a [Å]	18.3188(8)	7.4369(3)	13.921(3)
b [Å]	11.8244(3)	16.8946(6)	16.888(3)
c [Å]	7.8174(4)	12.0074(3)	7.6224(15)
α [°]	90	90	90
β [°]	116.210(6)	92.268(3)	120
γ [°]	90	90	90
V [Å^3]	1518.96(13)	1507.47(9)	1551.93
Z	4	8	4
μ [mm^{-1}]	0.354	0.357	
ρ_{calcd} [g cm^{-3}]	1.427	1.438	1.397
F [000]	680.0	680.0	680.0
θ [°]	4.244-52.734	4.164-52.736	3.38-27.60
T [K]	123.15	123.15	293(2)
R1	0.0255	0.0292	0.0500

wR2	0.0678	0.0790	0.1241
CCDC No.	745214	1987291	2070247

Computer simulation of BMeTTPAL molecule.

Conformer I   Conformer II   Conformer III   Conformer IV
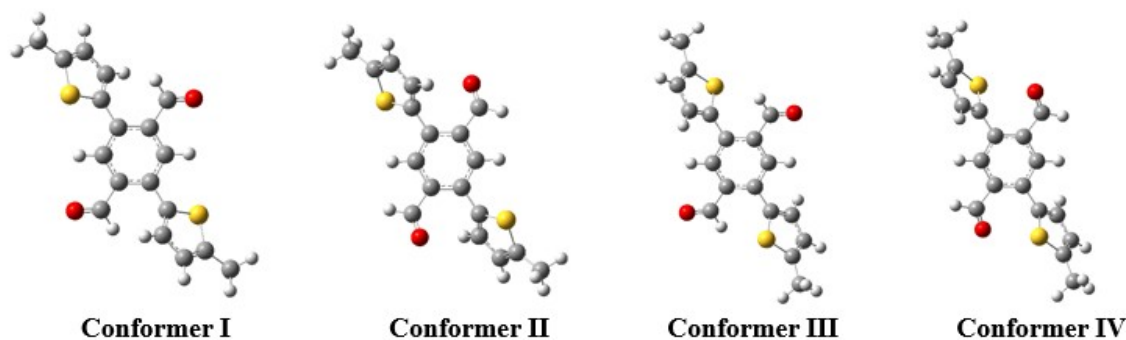
Fig. S10 Schematic diagram of different conformers of BMeTTPAL molecule in acetone. The energy of conformers, HOMO, LUMO and gap (LUMO-HOMO) can be seen in Table S5 and Figure S9. The calculation was based on M06-2X/6-311G(d,p) level and acetone was used as the solvent for calculations (Solvation Model Based on Density) at the M06-2X/6-311G(d,p) level.

Table S5. Energy data of different conformers of BMeTTPAL molecule.

| Solvents	I	II	III	IV
Toluene	-1641.025771	-1641.014536	-1641.023030	-1641.014188
1,4-Dioxane	-1641.018699	-1641.007077	-1641.015872	-1641.006693
Chloroform	-1641.027723	-1641.017350	-1641.024746	-1641.017572
Acetone	-1641.030041	-1641.020247	-1641.026791	-1641.020773
Acetonitrile	-1641.028984	-1641.019674	-1641.025648	-1641.020134

Note: The calculation was based on M06-2X/6-311G (d,p) level by Gaussian 09 software. Unit: Hartree.
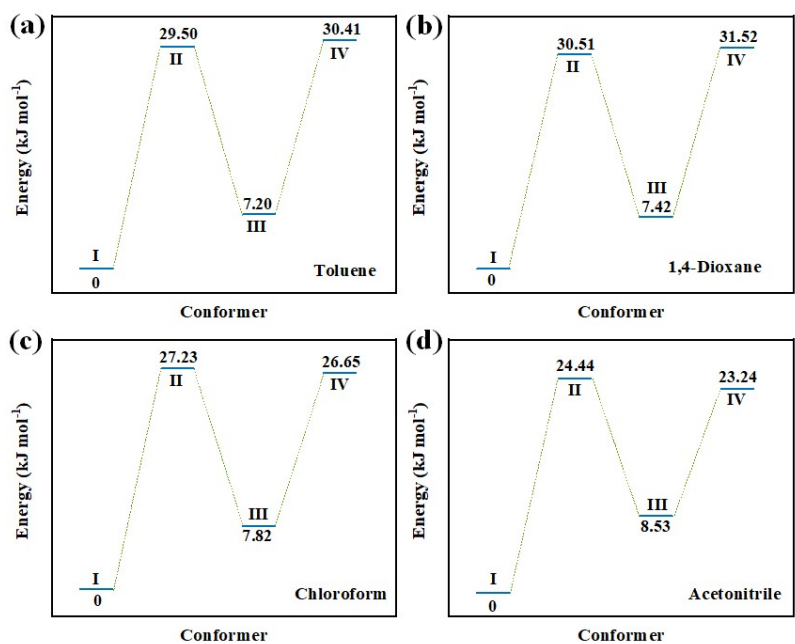
Fig. S11 (a) The diagram of energy of potential conformations of BMeTTPAL, the lowest energy of conformation I is set as 0 kJ mol^{-1} in different solvents.
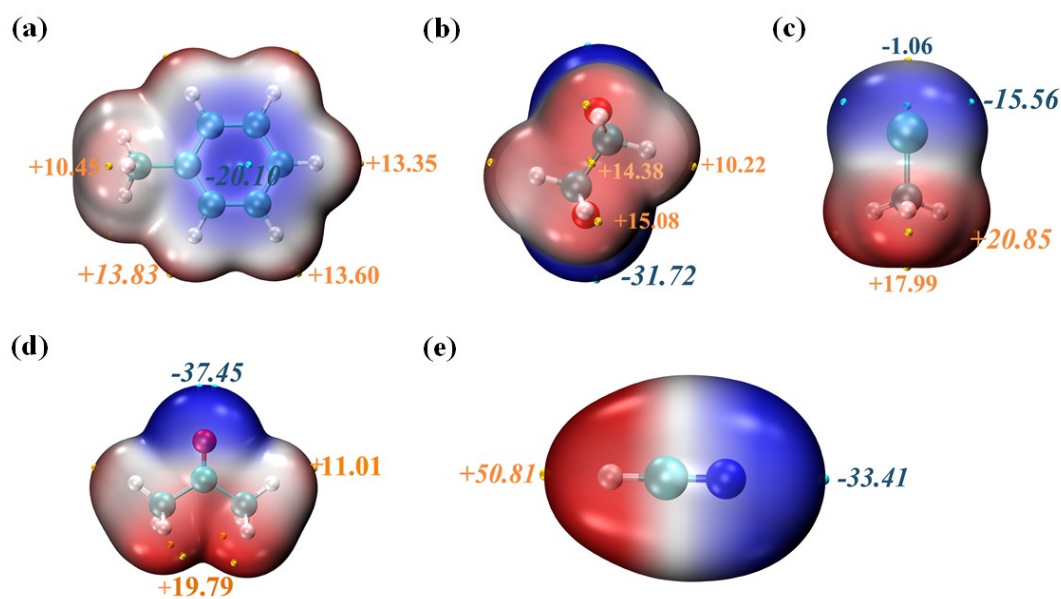
Fig. S12 ESP-mapped molecular vdW surface of solvent molecules: toluene (a), 1,4-dioxane (b), chloroform (c), acetone (d), acetonitrile (f). Surface local minima and maxima of ESP (units: kcal mol-1) are represented as cyan and orange spheres, respectively. The global minimum and maximum values are italic. The calculation was based on M06-2X/6-311G (d,p) level.[4-5]
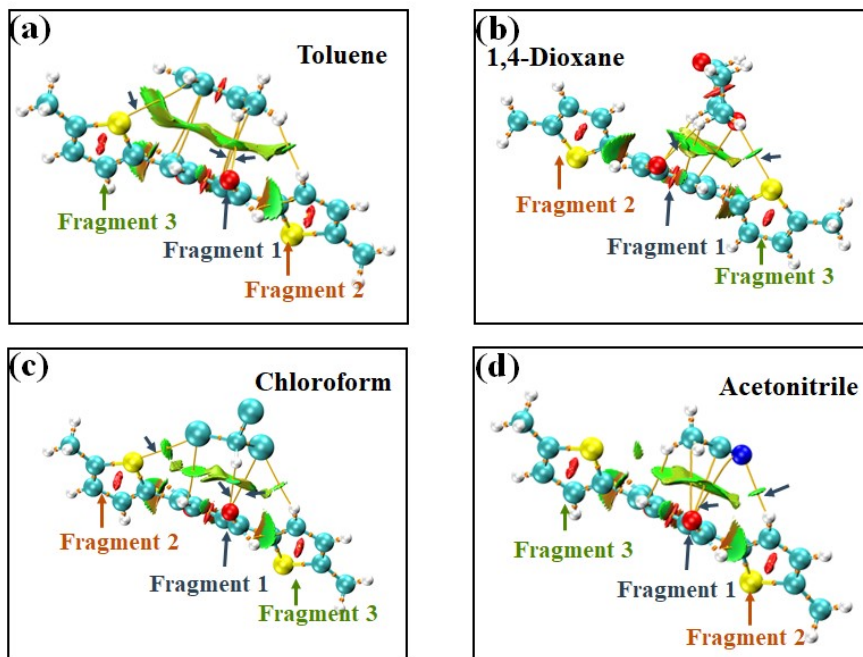
Fig. S13 The 1:1 complex of CA and toluene (a), 1,4-dioxane (b), chloroform (c), acetonitrile (d). Visualization in the molecular space of non-covalent interaction (NCI isosurfaces corresponding to RDG = 0.50 a.u.) and topological AIM graph in the dimer of CA and acetone. The orange lines represent the bond paths, the orange balls represent the bong critical points (BCPs).
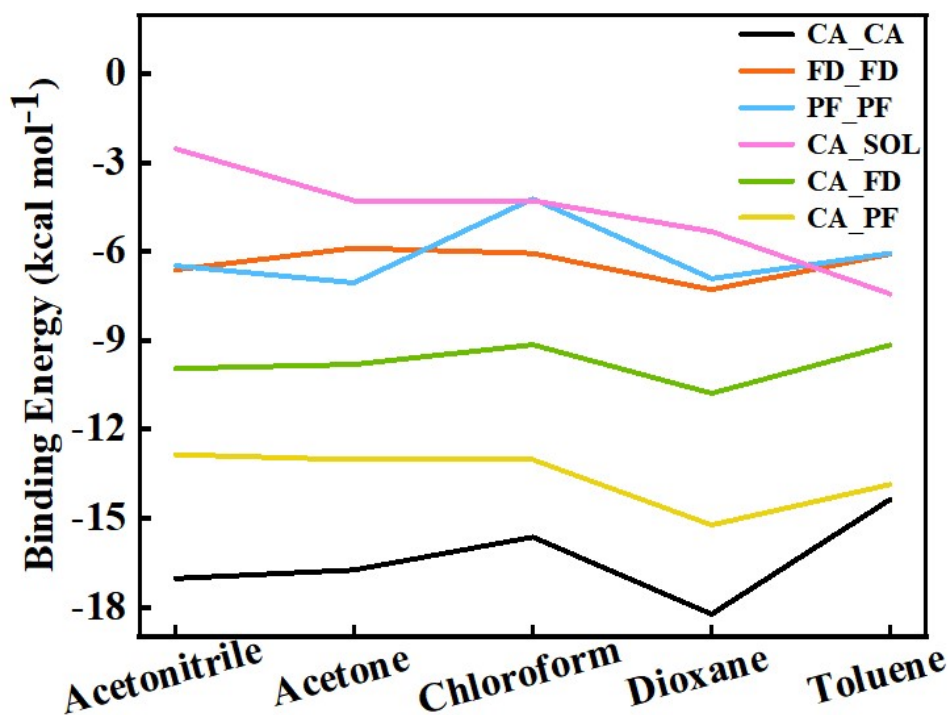

Fig. S14 The binding energy of 1:1 complex of CA_CA (black), FD_FD (orange), PF_PF (blue), CA_SOL (purple), CA_FD (green), CA_PF (yellow).

Table S6. The binding energy of 1:1 complex of CA_CA, FD_FD, PF_PF, CA_SOL, CA_FD, CA_PF.

| Sol	Toluene	1,4-Dioxane	Chloroform	Acetone	Acetonitrile
CA_CA	-14.36012337 967090	-18.23310183 328770	-15.63680407 213100	-16.74172716 165450	-17.03308437 556780
FD_FD	-6.078728124 77417	-7.285049755 27756	-6.054318072 71001	-5.877349115 10594	-6.613332929 24313
PF_PF	-6.054323140 09721	-6.909338852 79240	-4.216727928 19148	-7.050314076 36513	-6.475250243 33575
CA_SOL	-7.429105586 33591	-5.321273864 84570	-4.281371809 15833	-2.773370268 17350	-4.348454451 45129
CA_FD	-9.146966337 99917	-10.78589729 925070	-9.144256408 62374	-9.804530649 14504	-9.946364541 03890
CA_PF	-13.85707088 691300	-15.22403310 601880	-13.02568476 957070	-13.02330613 453390	-12.85043788 373980

Note: The calculation was based on M06-2X/6-311G (d,p) level by Gaussian 09 software. Unit: kcal mol^{-1}.
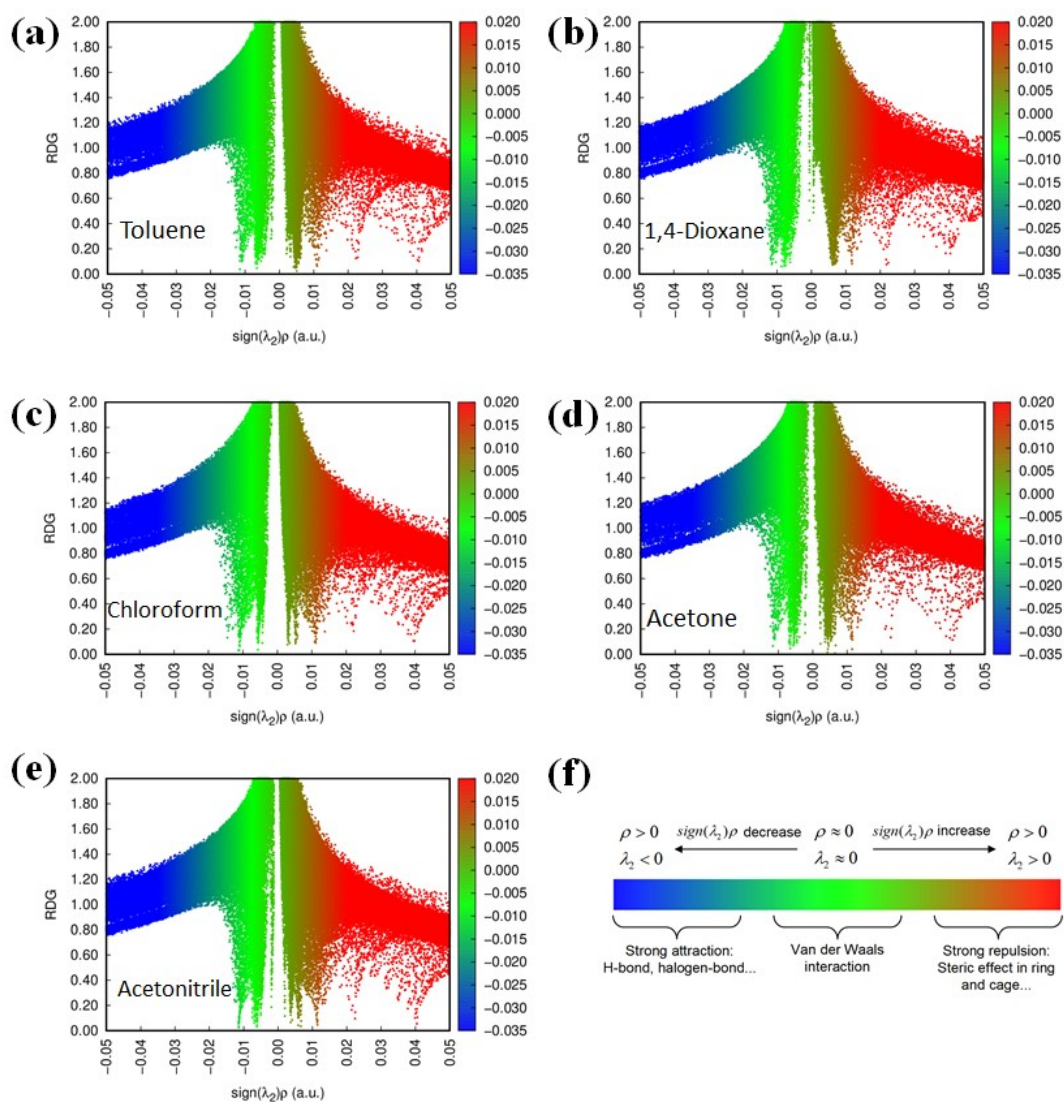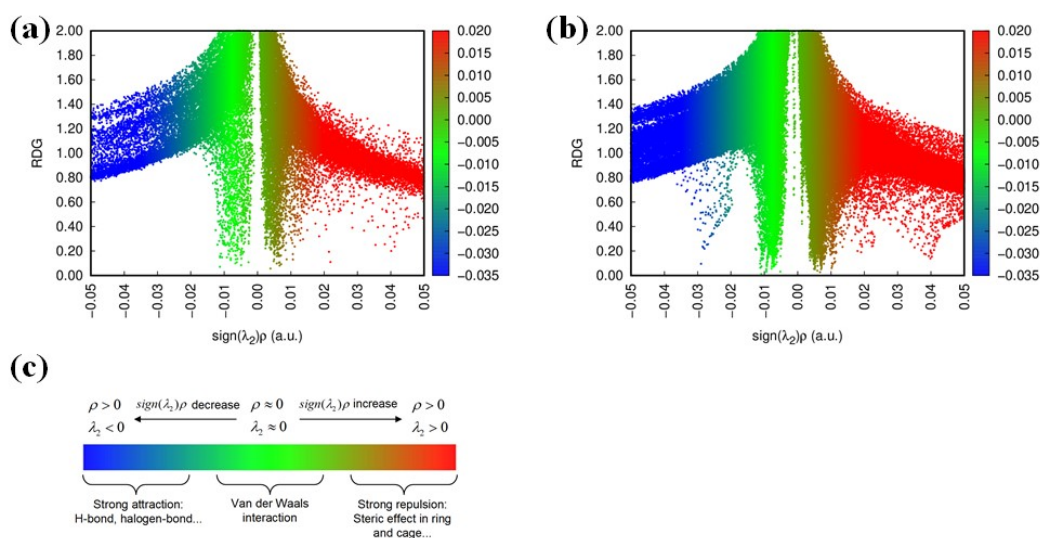
Fig. S15 Scatter map of non-covalent interaction (NCI) of CA and toluene (a), 1,4-dioxane (b), chloroform (c), acetone (d), acetonitrile (e); Color scale bar related to the color-filled NCI (RDG) isosurface in Fig S10 and Fig S11.
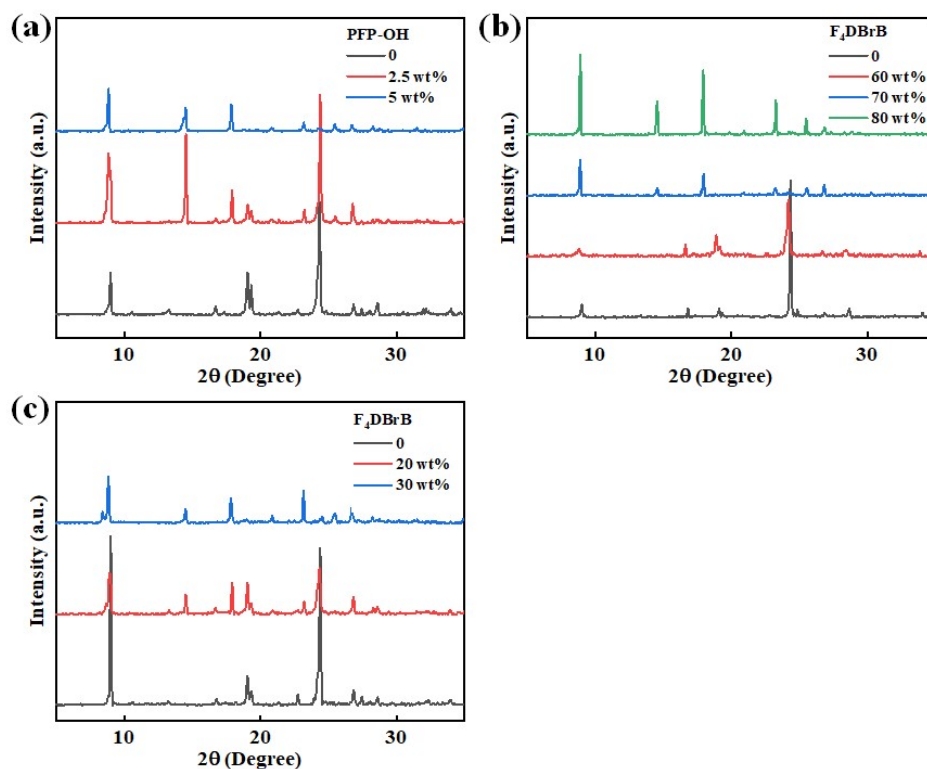
Fig. S16 (a) The PXRD patterns of CA with different concentrations of PFP-OH in acetone in the cooling crystallization process; (b) The PXRD patterns of CA with different concentrations of F_4DBrB in acetone in the evaporation crystallization process; (c) The PXRD patterns of CA with different concentrations of F_4DBrB in acetone in the cooling crystallization process.
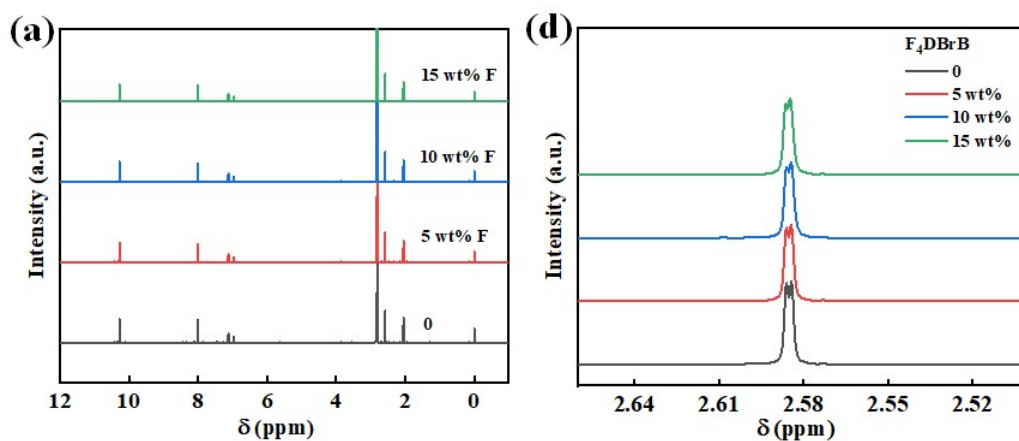
Fig. S17 (a) The ^1H NMR spectra of CA in d^6-acetone with different concentrations of PFP-OH; (b) Partial enlarged view of (a).

Fig. S18 Scatter map of non-covalent interaction (NCI) of CA and F4DBrB (a), PFP-OH (b); Color scale bar related to the color-filled NCI (RDG).
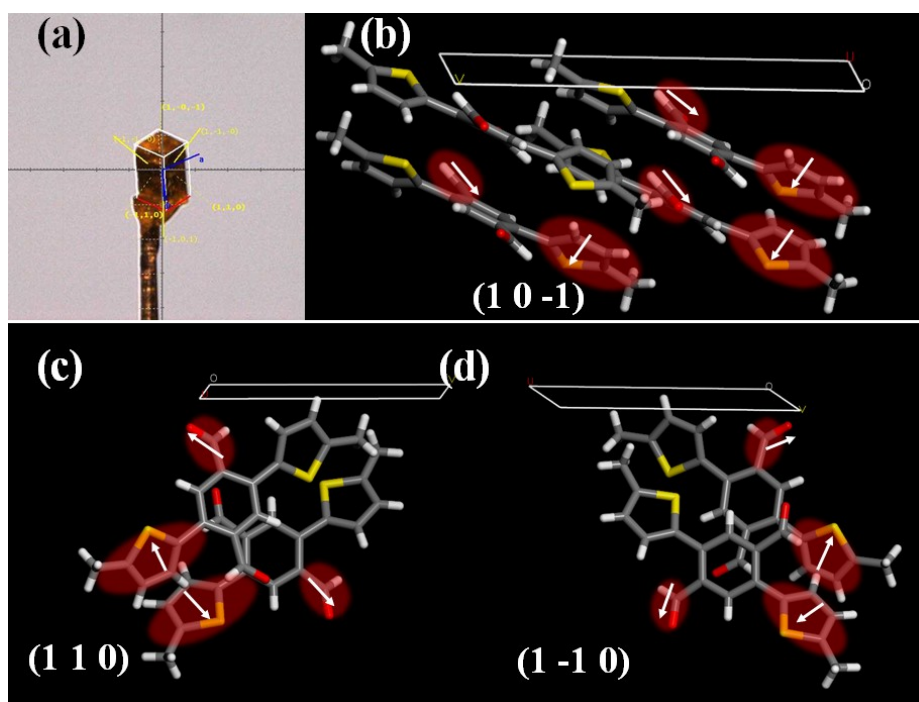
Fig. S19 (a) Single crystal of Form I with Miller indices of observable faces; (b-d) molecular arrangement in crystal surfaces of (10-1), (110) and (1-10). The red ellipses represent EDG and EWG with large torsion angles, and the white arrows represent the orientation of S and O atoms.
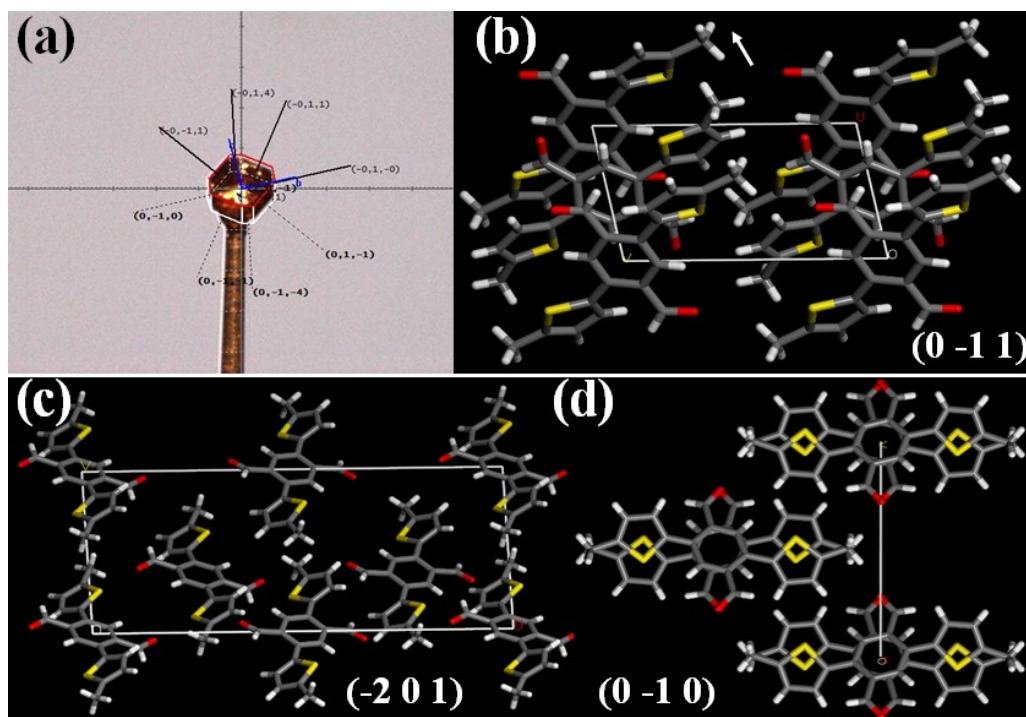
Fig. S20 (a) Single crystal of Form II with Miller indices of observable faces; (b-d) molecular arrangement in crystal surfaces of (0-11), (-201) and (0-10).

Reference

1 Pietrangelo, A., Patrick, B. O., MacLachlan, M. J., Wolf, M. O., *J. Org. Chem.,* 2009, **74**, 4918–4926.

2 Miao, D., Daigle, M., Lucotti, A., Boismenu-Lavoie, J., *Angew. Chem. Int. Ed.,* 2018, **57**, 3588–3592.

3 Zhang, X. N., Wang, J. K., Liu, Y., Hao, Y. H., Yu, F., Li, D. N., Huang, X., Lu, Y., Wang, T., Hao, H. H. Tunable Emission of Organic Fluorescent Crystals through Polymorphic Manipulation. J. Phys. Chem. C, 2021, 125, 6189–6199.

4 Lu, T., Chen, F., Multiwfn: a multifunctional wavefunction analyzer. *J. Comput. Chem.* 2012, **33**, 580–592.

5 Tian Lu, Multiwfn Manual, version 3.6(dev), Section 3.21.1, available at http://sobereva.com/multiwfn (accessed Aug 30, **2018**).